

# Perceived Annoyance to Noise Produced by a Distributed Electric Propulsion High Lift System

Dan Palumbo<sup>1</sup>, Jonathan Rathsam<sup>2</sup>, and Andrew Christian<sup>3</sup>  
*NASA Langley Research Center, Hampton, VA, 23681*

and  
Menachem Rafaelof<sup>4</sup>  
*National Institute of Aerospace, Hampton, VA, 23666*

## I. Abstract

Results of a psychoacoustic test performed to understand the relative annoyance to noise produced by several configurations of a distributed electric propulsion high lift system are given. It is found that the number of propellers in the system is a major factor in annoyance perception. This is an intuitive result as annoyance increases, in general, with frequency, and, the blade passage frequency of the propellers increases with the number of propellers. Additionally, the data indicate that having some variation in the blade passage frequency from propeller-to-propeller is beneficial as it reduces the high tonality generated when all the propellers are spinning in synchrony at the same speed. The propellers can be set to spin at different speeds, but it was found that allowing the motor controllers to drift within 1% of nominal settings produced the best results (lowest overall annoyance). The methodology employed has been demonstrated to be effective in providing timely feedback to designers in the early stages of design development.

## II. Introduction

Compared to either turbine or internal combustion propulsion systems, electric motors, in general, provide greater flexibility in control of propeller rotation rate (rpm). In the context of a Distributed Electric Propulsion (DEP) design, the question arises as to whether the additional degrees of freedom provided by the electric motors can be used to reduce perceived annoyance to the aircraft's sound experienced by people on the ground as the aircraft passes overhead. For example, would setting the distributed motors to spin at slightly different rpm rather than one single rpm significantly reduce peak sound levels thereby reducing annoyance? Following this train of thought, the auralization group in NASA Langley's Structural Acoustics Branch was tasked to model and evaluate the perceived annoyance of different configurations of a high lift system proposed as part of the Leading Edge Asynchronous Propellers Technology Project (LEAPTech) [1] [2]. A LEAPTech design concept with 8 high-lift propellers and two cruise propellers is shown in Figure 1.

---

<sup>1</sup> AST, Flight Vehicle Acoustics, Structural Acoustics, MS 463, and member AIAA.

<sup>2</sup> Research AST, Structural Acoustics, MS 463.

<sup>3</sup> Research AST, Structural Acoustics, MS 463, and AIAA Member.

<sup>4</sup> Sr. Research Engineer, 1000 Exploration Way.

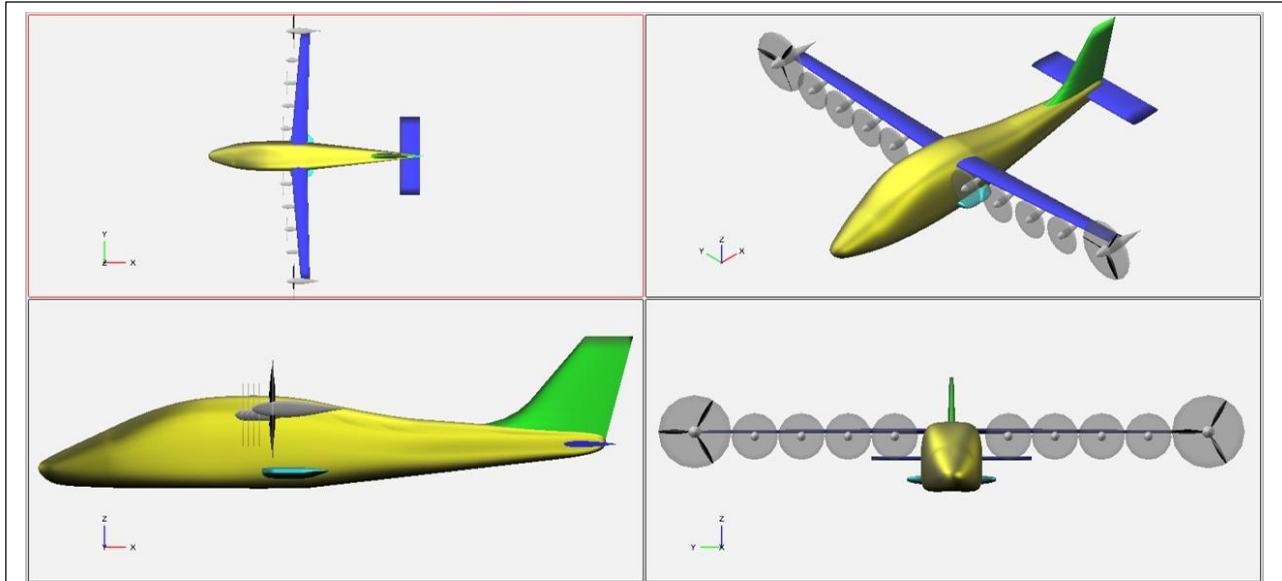


**Figure 1. LEAPTech concept with 8 high-lift propellers.**

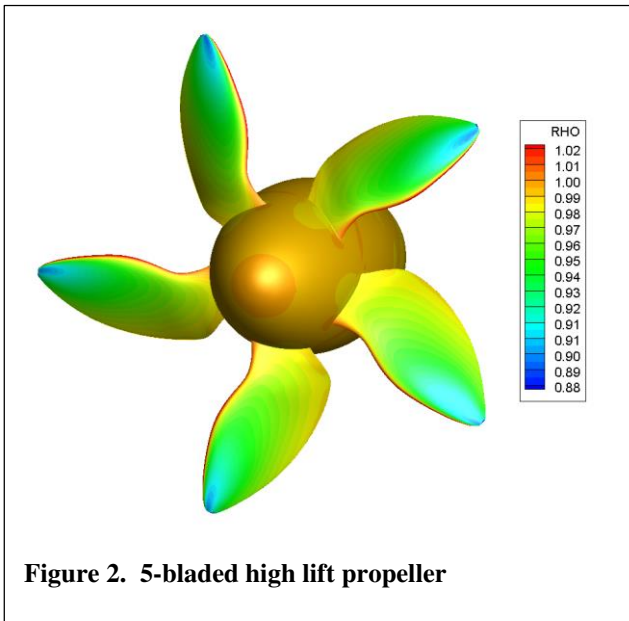


**Figure 2. 5-bladed high lift propeller**

To augment lift, the propellers are designed to produce a maximum increase in the velocity of air ( $\Delta V$ ) per unit power while minimizing tip speed. Tip speed is a major factor in noise production as will be explained in the following section. This design goal leads to an unconventional shape for the propeller, see Figure 2. Additional constraints on propeller design were that the tip speed be held constant and that the blades be able to fold away during cruise.

Sound metrics exist which predict annoyance, but they cannot be relied upon when applied to new sound sources due to the highly subjective nature of annoyance. Instead, a psychoacoustic test is conducted where subject responses to representative sounds are obtained (for example see [3]). In this paper the LEAPTech design space relevant to the psychoacoustic test will be introduced, the auralization and synthesis methods used to produce the sounds will be described, the psychoacoustic test philosophy and test plan design will be explained, and, the results presented and discussed.

### III. LEAPTech Psychoacoustic Design Parameters

In general, Loudness [4] is the most influential acoustic predictor of sound's perceived annoyance. The Loudness metric is derived from the power spectrum of the source sound emission and is frequency dependent due, primarily, to the ear's non-constant frequency response. In the case of a propeller, the total sound power emitted is proportional to the 5<sup>th</sup> power of the propeller tip speed [5]. The propeller tip speed is, in turn, dependent on its diameter and rpm. In the LEAPTech design space, the diameter of the high lift propellers is constrained by the wingspan for a given number of propellers (NP). The tip speed is constrained to be the same regardless of diameter to ensure adequate airflow. Keeping the wingspan constant, setting NP will place an upper limit on the propeller diameter, and, once the diameter is set, the rpm at which the propeller must spin to produce the air flow required to generate the desired lift augmentation. The number of propellers, NP, influences the propeller diameter, its blade passage frequency (BPF) and the propeller tip speed. NP is then seen as a primary design parameter of the high lift system influencing the perceived annoyance through total sound power emitted and that power's frequency distribution.

In the simplest design all the propellers would be spinning at the same rpm with the effect that the sound power would be concentrated at the propeller's BPF and harmonics producing highly tonal sound at increased levels. This would be perceived, potentially, as very annoying. The nature of the sound can be changed by setting the propellers to different rpm. This configuration has been termed 'spread frequency'. In a spread frequency design the sound power would be distributed over several BPFs and their associated harmonics thereby changing the nature of the sound as well as the spatial distribution of the sound power over the landscape. Spatial radiation patterns of mean square pressure are shown in Figure 3 for an aircraft with 12 propellers located in the center of 1 sq. km and traveling from left to right at an altitude of 330 m. This configuration is used to produce results in all figures where synthesized sound is presented. A single rpm configuration is compared to that of a spread frequency configuration. The phase coherence in the single rpm design produces a highly focused interference pattern with the highest levels of sound pressure level (SPL) along the centerline, Figure 3, left. There is no coherence between the propellers' emissions in the spread frequency design, Figure 3, right. The peak sound level along the centerline is down approximately 10 dB compared to peak single rpm levels with the SPL spread more uniformly over the area. This would, however, potentially expose more people to somewhat higher levels than in the single rpm case. It should be noted that the total sound power over the area is conserved in both designs.

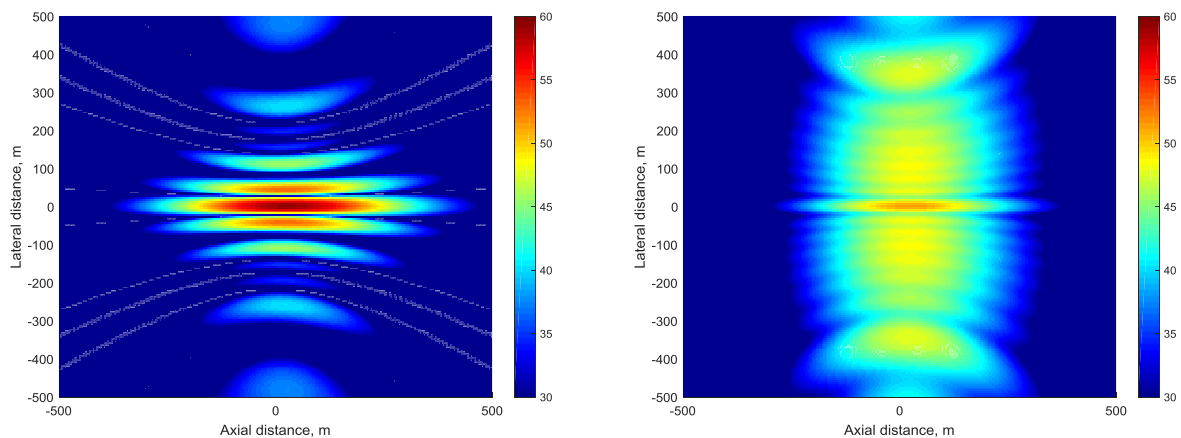
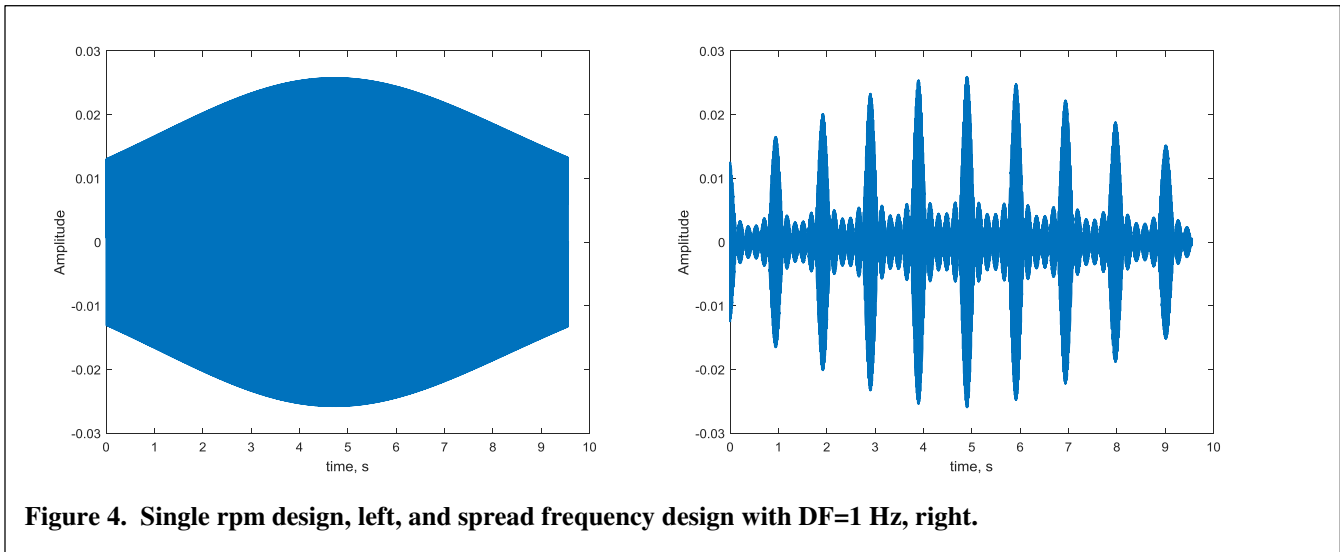
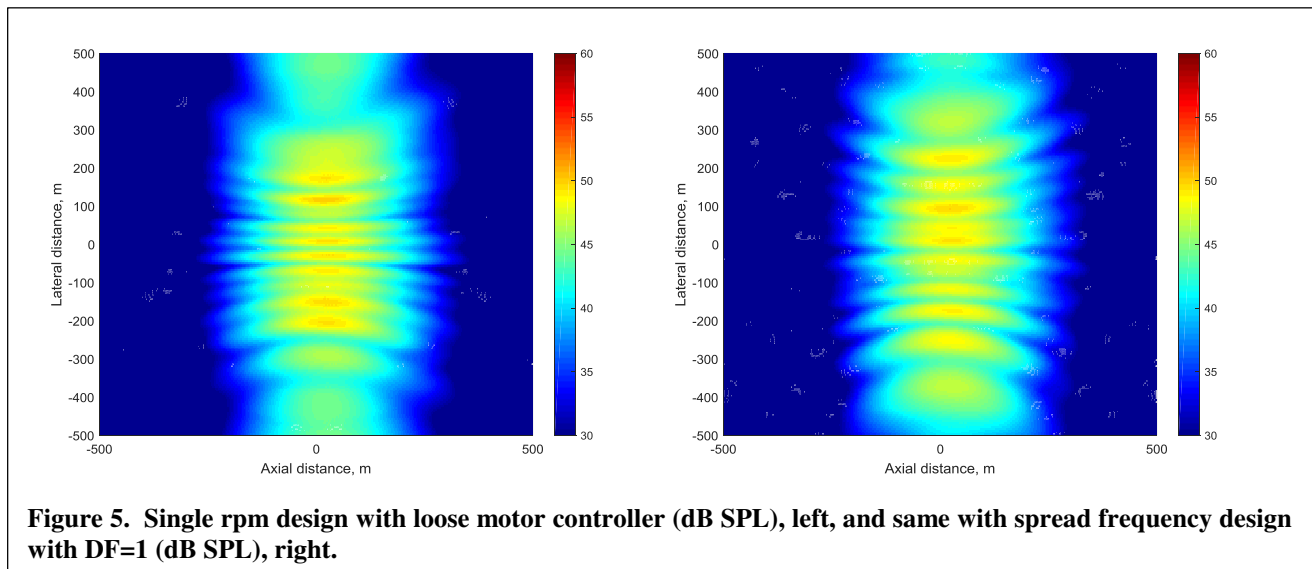


**Figure 3. Single rpm pressure distribution (dB SPL), left. Spread frequency pressure distribution (dB SPL), right.**

Any reductions in sound level and tonality gained in the spread frequency design may be a benefit, but could just as well be detrimental, introducing modulation (or beating) which could increase annoyance. This is illustrated in Figure 4 which displays the noise envelope produced during a flyover. In the single rpm design, Figure 4, left, the sound envelope smoothly increases and decreases as the aircraft passes overhead. In the spread-frequency design with a difference of 1 Hz between adjacent propeller BPFs, the sound envelope is modulated at 1 Hz with a high depth of modulation, Figure 4, right. To better understand this tradeoff, a second design parameter, delta frequency (DF), is introduced to define the frequency step between adjacent propeller BPFs. The frequency step is constrained by system design considerations to keep the propeller rpm to within +/- 5% of its design value.



How well a sound synthesized using the NP and DF parameters models reality is dependent in part on the steadiness of the propellers' rpm in flight. For example, any drifting of propeller rpm will introduce phase variance that reduces coherence between the propellers' sounds thereby reducing the degree of modulation produced by the interference between the sounds. Ignoring, for the time being, external factors, such as refraction and reflection, any inconsistency in propeller rpm can be related to the performance of the motor controller. The controller can be 'loose', keeping rpm to within 1% of specification, or, 'tight', keeping rpm to within 0.1% of specification. A single rpm design with loose motor controllers produces a spatial SPL distribution similar to that of a spread frequency design, Figure 5, left. Adding spread frequency smooths the spatial distribution somewhat but has little effect on sound pressure levels, Figure 5, right.



Motor control error can have a profound effect on the sound. A loose controller can cause a high degree of modulation in the single rpm design as can be seen in Figure 6, left. The sound heard with perfect control, Figure 4, left, will be very different from that heard with a loose controller, Figure 6, left. A loose control with a spread frequency design, Figure 6, right, appears similar to the single rpm design but with a higher frequency of modulation. The controller error is modeled by a constant frequency offset and sinusoidal variation about the offset. This model was adopted after examining controller data taken from a stationary ground test. Specifically, the frequency offset is modeled by an error term,  $f_e$ , and the modulation of the frequency by a phase magnitude,  $\phi$ , and modulation frequency,  $f_\phi$ .

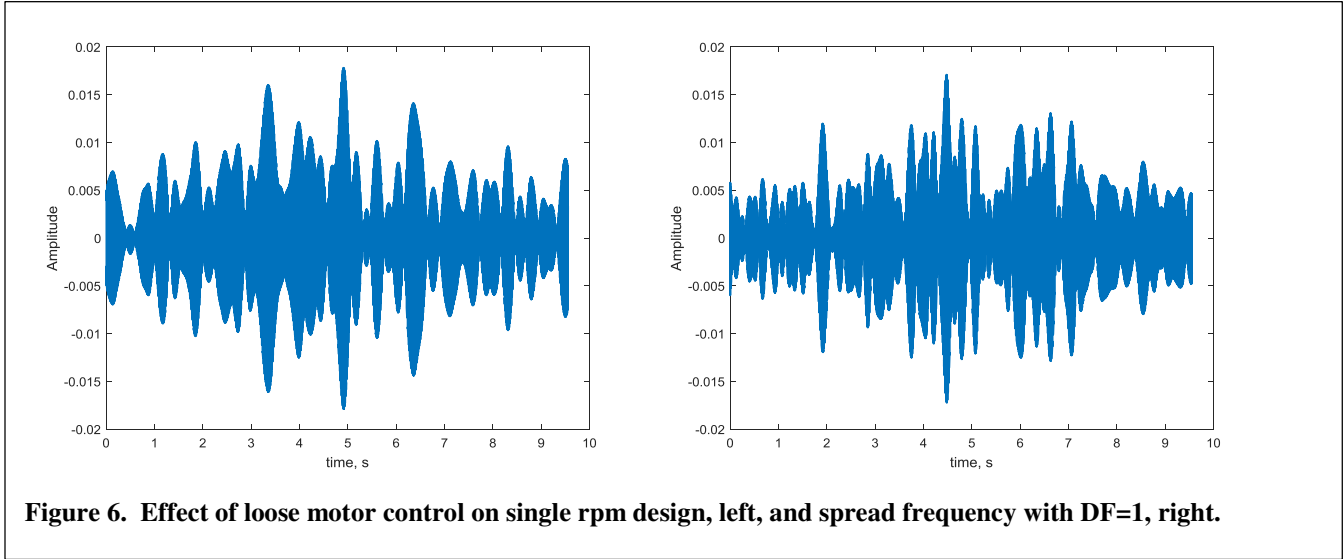


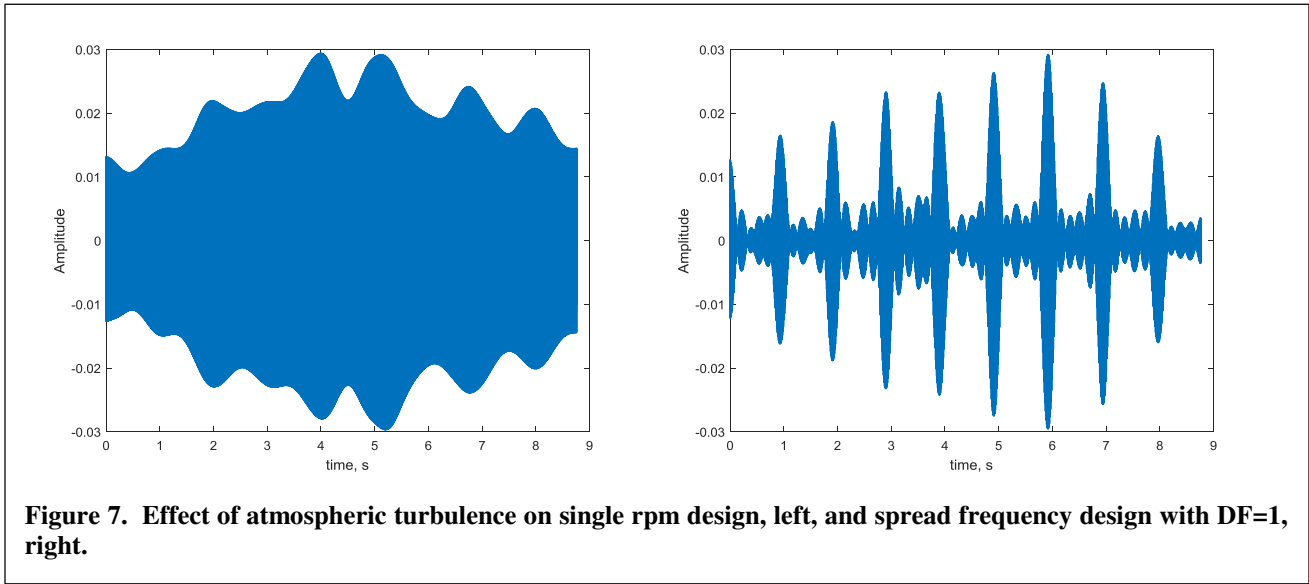
**Figure 6. Effect of loose motor control on single rpm design, left, and spread frequency with DF=1, right.**

A final consideration related to motor control is propeller phase synchronization. Phase synchronization is possible when all the propellers are at the same rpm (DF = 0) but not under spread frequency conditions (DF > 0). The initial propeller phase is modeled by parameter  $\theta$  and is set randomly during synthesis when DF > 0.

#### IV. Atmospheric Turbulence Parameters

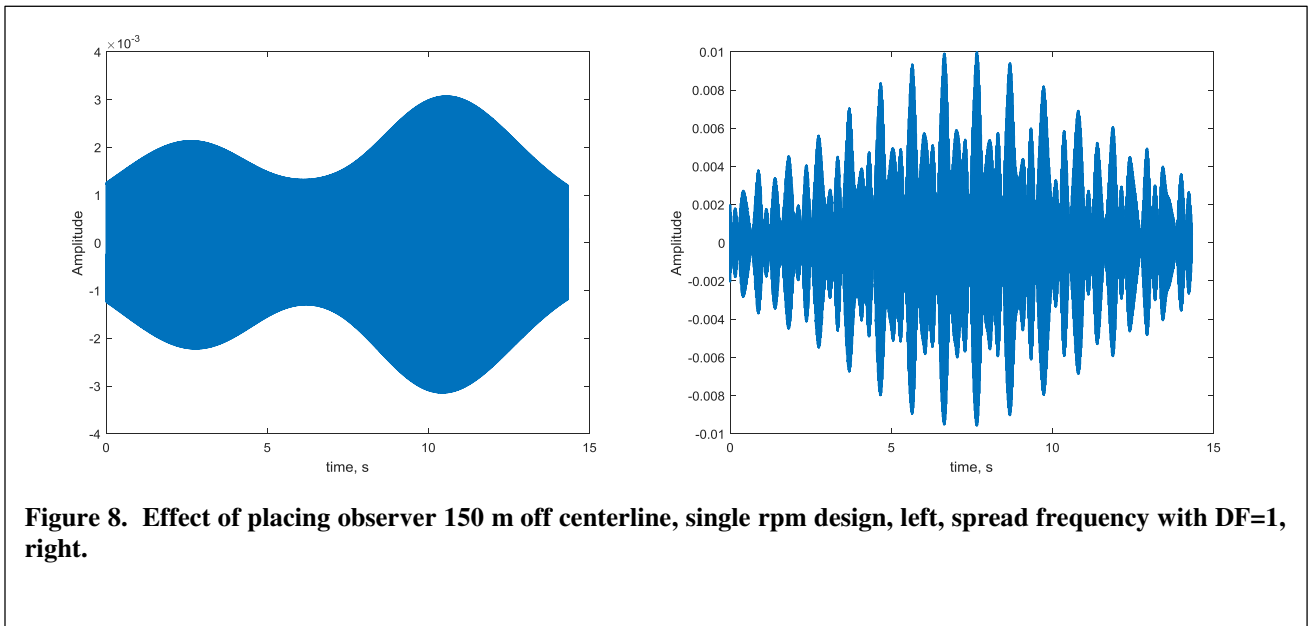
As referred to in the motor controller discussion above, the synthesized sound fidelity with respect to what one might hear in reality is dependent on the coherence of the distributed sources at the listener's ears. In addition to the *incoherence* contributed by the motor controller, atmospheric turbulence can greatly influence both the amplitude and phase of propagating sound.

There are at least two ways in which atmospheric turbulence can perturb the sound character. First, it can directly affect the source by varying the load on the propeller. This effect was not modeled. Second, it can refract the sound waves changing the sound propagation path thereby introducing variance into both the amplitude and phase of the sound. Ostashev [6] has published graphs that predict normalized log-amplitude and phase variances given a dimensionless wave parameter, D. The normalization factors depend on the frequency of the sound, the altitude and distance of the source and the Mach number of the turbulence. Using given test conditions (see Section VI) and assuming a Gaussian distribution, the log-amplitude variance,  $\alpha$ , and phase variance,  $\psi$ , can be applied to the sound during synthesis. The effects of nominal atmospheric turbulence are shown in Figure 7. The envelope of the single rpm design exhibits a fair degree of modulation, Figure 7, left. A similar degree of amplitude modulation is shown for the spread frequency design, Figure 7, right. The depth of modulation caused by the beating of one propeller's emission against another's is phase sensitive. This effect can also be seen in Figure 7, right.



### V. Location of the Observer

As described above, the phase relationship between the multiple sources will affect the degree and frequency of modulation an observer on the ground will hear. In addition to motor controller error and atmospheric turbulence, the location of the observer will influence the phasing of the sounds the observer experiences due to changing propagation path lengths as the aircraft is moving. If the observer is on the centerline of the aircraft's trajectory, that is, the aircraft is passing directly overhead, the sources will be symmetrically spaced relative to the observer making the path lengths between symmetric pairs of propellers on the wings the same. The rpm (and, therefore, BPF) of symmetric pairs of propellers is, under most conditions, set the same to eliminate yawing forces. As the path lengths and frequencies of the symmetric pairs are the same on centerline, the sound will appear to be coming from a single central source with no modulation or beating induced between symmetric pairs.



Contrast this to an observer on the sideline, Figure 8. In this case the path lengths from each propeller change depending on its unique position on the wing. This will introduce phase changes between symmetric pairs that would not occur if the observer were on the centerline. The effect in the single rpm case is a slow amplitude modulation of the waveform, Figure 8, left. In the spread frequency case there is a bifurcation of the secondary lobes, Figure 8, right. These effects may seem subtle, but they will be quite audible and will likely influence perceived annoyance.

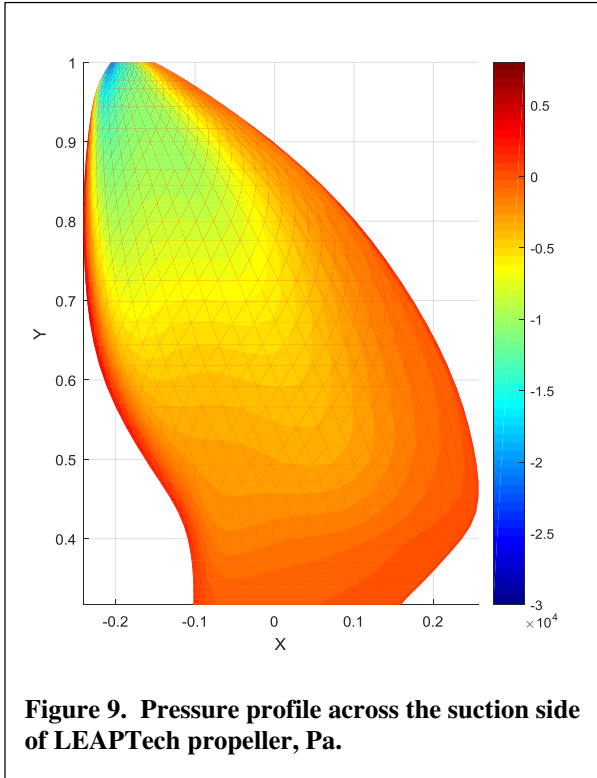


Table 1. Synthesis parameters

Parameter	Definition
$f_i$	Blade passage frequency of propeller $i$
$n$	Harmonic number
$\theta$	Initial phase of propeller $i$
$f_{ei}$	Frequency offset error of propeller $i$
$\phi$	Time varying phase amplitude
$f_\phi$	Frequency of time varying phase (5 Hz)
$\varphi$	Phase offset of propeller $i$ time varying phase
$\alpha(t)$	Amplitude modulation turbulence
$\psi(t)$	Phase modulation turbulence

## VI. Sound Synthesis

The noise the propeller produces is derived from predictions of sound radiation that has as its source the rotating blade surface pressures, Figure 9. The blade surface pressures can be obtained using either CFD or the Propeller Analysis System [7] that is part of the NASA Aircraft Noise Prediction Program, ANOPP. The radiating sound pressures are predicted from the blade pressures using the F1A module of ANOPP2 [8]. This process is shown as a block diagram in Figure 10.

Sound pressure predictions are made on a hemisphere to provide for synthesis along any combination of elevation and azimuthal angles. The hemispheres are generated at a sample rate adequate to resolve the harmonics in the blade pressures. Enough samples to encompass one complete blade passage are computed. The hemisphere predictions for one blade passage are repeatedly sampled to fill the specified flight time. The predictions for this test were made at a propeller angle of attack of 0 degrees and did not include installation effects such as propeller-to-propeller and propeller-to-structure interactions. The blade surface pressure predictions were based on the LEAPTech propellers, which were designed specifically for low tip speed. For these reasons, the predicted sound had few significant harmonics. This made it possible to synthesize the sound using simple sine functions whose amplitude, frequency and phase were determined by the parameters described in previous sections and listed in Table 1.

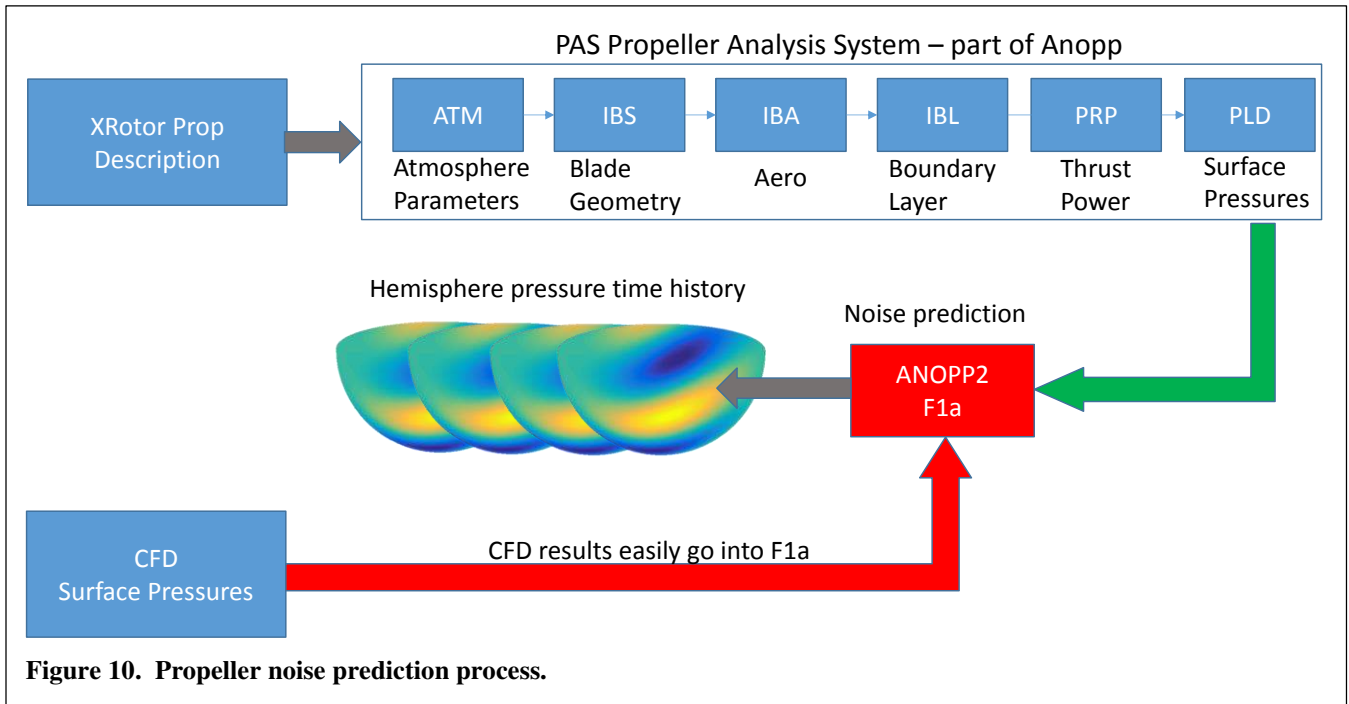


**Figure 10. Propeller noise prediction process.**

In ideal conditions without any other effects, the radiated acoustic pressure of the  $i^{\text{th}}$  propeller,  $p_i$ , can be defined as

$$p_i(t) = \frac{\sin(2\pi n f_i t)}{r_i} \quad (1)$$

where  $f_i$  is the blade passage frequency (BPF),  $n$  is the harmonic number and  $r_i$  is the distance from the propeller to the observer. The  $r_i$  describe a straight-line path from source,  $i$ , to the observer. Reflections and refractions are ignored. This form of the synthesis assumes that all the propellers are synchronized and start at the same phase angle. If the propellers are not synchronized, a random phase offset,  $\theta_i$ , is added to the synthesis model with  $\theta_i \neq \theta_j$ .

$$p_i(t) = \frac{\sin(2\pi n f_i t + \theta_i)}{r_i} \quad (2)$$

Motor controller error manifests itself as a constant frequency offset,  $f_{ei}$ , and a time varying phase,  $\phi_i(t)$ .

$$p_i(t) = \frac{\sin(2\pi n (f + f_{ei}) t + \theta_i + \phi_i(t))}{r_i} \quad (3)$$

where

$$\phi_i(t) = 2\pi \phi \cos(2\pi f_\phi t + \varphi_i) \quad (4)$$

In Eq. 3  $f_{ei} \neq f_{ej}$  and  $\phi_i(t) \neq \phi_j(t)$ . The  $\phi_i$  are made unique by the addition of random offset,  $\varphi_i$ . Time varying amplitude modulation,  $\alpha(t)$ , and phase modulation,  $\psi(t)$  are added to simulate realistic atmospheric conditions.

$$p_i(t) = \frac{\alpha(t) \sin(2\pi n (f_i + f_{ei}) t + \theta_i + \phi_i(t) + \psi(t))}{r_i} \quad (5)$$



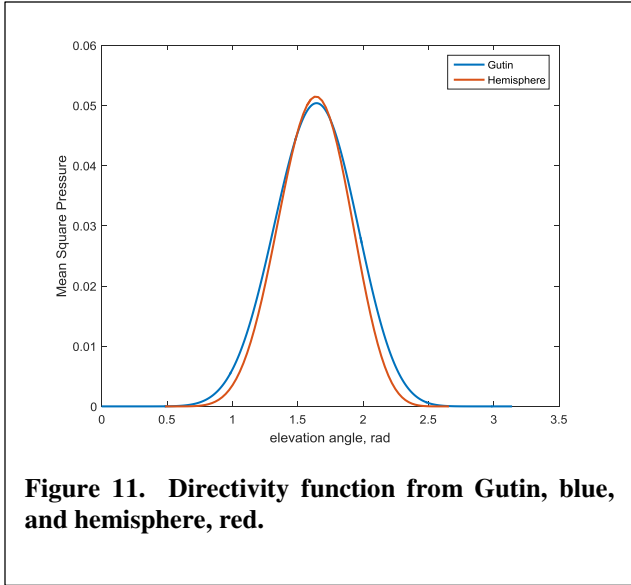


**Figure 11. Directivity function from Gutin, blue, and hemisphere, red.**

In addition to the analytical prediction represented by Eq. (5), a prediction or estimate of the propeller’s directivity is necessary to scale the magnitude of the emission as the source moves overhead and the emission angle changes. It was found that the prediction given in Gutin [9] closely matches the directivity implicit in the hemisphere prediction produced by ANOPP2 F1A, Figure 11.

The propellers were set to cruise at an altitude of 300 m and a velocity of 31 m/s. The propeller settings on one span were the mirror image of those on the other with the highest rpm located inboard. All the parameters in the numerator of Eq. 5 can have some component of randomization across the propeller array as will be explained in the next section.

### VII. The Psychoacoustic Test

A psychoacoustic test exposes human test subjects to sounds and records their reactions. The test is designed to quantify the metric of interest, which, in this case, is annoyance. The sounds were designed to span the NP by DF design space with the underlying test matrix illustrated in Figure 12. The number of propellers, NP, was either 6, 12 or 18, which corresponds to blade passage frequencies of 161, 322 and 483 Hz. The delta frequency step was 0, 1, 3 or 5. The maximum DF of 5 was determined by the constraint to keep the propeller rpm to within +/- 5% of its design specification. A third dimension to the test matrix was tight vs. loose control. It was observed in early synthesis trials that the sounds generated by a loose controller were often less annoying. The downside to the loose controller was that the outcome is unpredictable. The sounds could just as well be very annoying. To test if the attributes of a loose controller could be emulated by a tight controller, a set of sounds was generated using a tight controller with randomized DF.

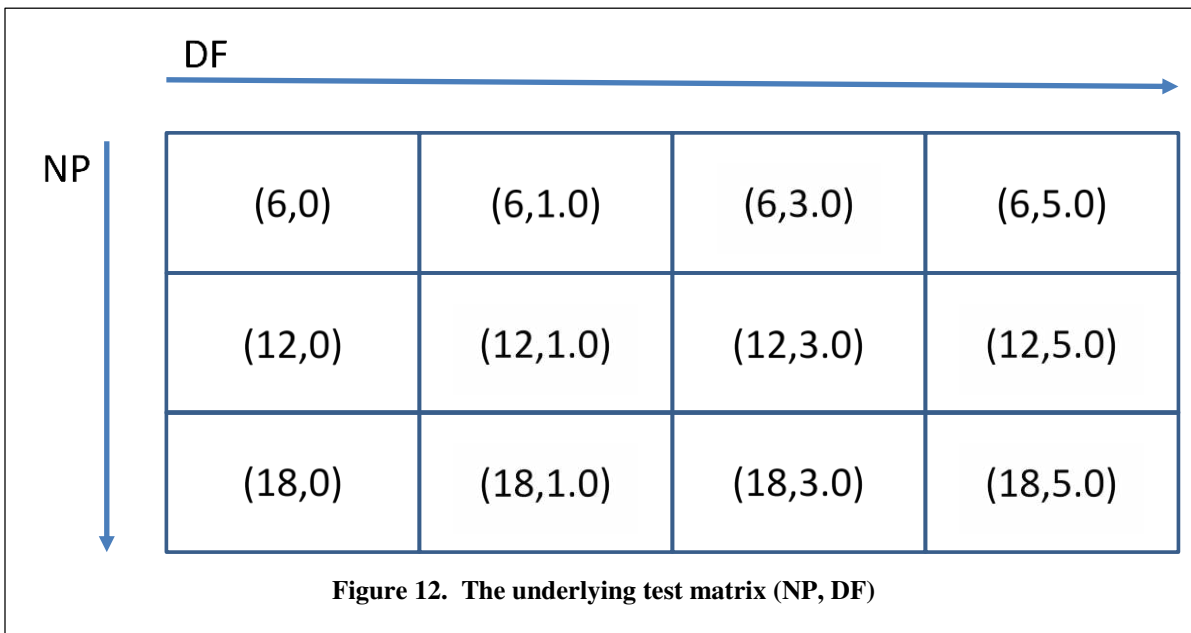


**Figure 12. The underlying test matrix (NP, DF)**

The beating induced in spread frequency configurations is dependent on the relative phasing of the sources. Most of the sounds were generated with the observer on the centerline, that is, directly beneath the sources, so that the phases from the mirrored sources on each span were equal. This results in very predictable sound patterns. If one were to move off the centerline, the phase alignments would be quite different, resulting in very different sounds. To test this effect, sounds were also generated with the observer on the sideline, 150 m off centerline. In all, 5 classes of sounds were synthesized, Table 2.

Examples of sounds from 3 of the 5 classes are shown in Figure 13 (Ideal sounds are shown in Figure 4 and sideline sounds do not appear, visually, to be much different from the Realistic sounds). In Figure 13, the left hand column contains sounds synthesized with a single rpm (DF=0). The right hand column contains spread frequency sounds (DF=1). Graphs (a) and (b) are Realistic class. The motor controller is tight ( $f_{ei}$  and  $\phi$  set to 0.1% variance), there is random initial phase and amplitude

**Table 2. Sound Classes**

Class	Control	Initial Phase	Turbulence	Location	DF
<b>Ideal</b>	Perfect	0	none	centerline	as set
<b>Realistic</b>	tight ( $f_{ei}$ and $\phi$ 0.1% of setting)	random	yes	centerline	as set
<b>Sideline</b>	tight	random	yes	150 m off center	as set
<b>Random DF</b>	tight	random	yes	centerline	randomized
<b>Loose Control</b>	loose ( $f_{ei}$ and $\phi$ 1% of setting)	random	yes	centerline	as set

and phase variation due to atmospheric turbulence is applied. The effects of atmospheric turbulence are most apparent in this class. Graphs (c) and (d) are Loose Control class ( $f_{ei}$  and  $\phi$  1% variance). The loose motor control seems to have the most apparent effect on (c) the single rpm, DF=0, design. Loose control induces more high frequency modulation in the spread frequency design. The Random DF class does not have a sound sample for the single rpm design (DF=0). The spread frequency design (e) exhibits very high frequency modulation, which will be shown to be more annoying than the Loose Control case.

All the sound classes except for Ideal have random parameters. The randomized setting of these parameters greatly influences the character of the sound. As it is not feasible to perform an exhaustive test of the randomized parameters for all the classes, a scheme was employed by which 2 sounds were selected from each randomized class. The scheme utilized the sound metrics Loudness and Depth of Modulation<sup>5</sup> as these were judged to be sensitive to the permutations being applied to the sounds. Thirty randomized sounds were generated for each class. The sounds were ordered and scored according to their respective metrics weighting Loudness scores twice that of Depth of Modulation scores. The sounds with the highest and lowest scores were selected from each class. This would have resulted in a complete matrix of 120 sounds (12\*5\*2). However, some elements in the matrix were not included. For example, the Ideal class is not randomized (12 fewer sounds). Ideal single rpm (DF=0) sounds were not tested as it was thought that this purely tonal case would be so much more annoying than the other cases that the response range of the remaining classes would be compressed reducing the ability to discriminate between the classes results (3 fewer sounds). Random DF class DF=0 elements was not tested as this class does not apply to the DF=0 case (6 fewer sounds). With these adjustments, the test suite contained 99 sounds.

The goal of the LEAPTech psychoacoustic test was to inform distributed electric propulsion system design by providing a prediction of the public’s annoyance to the sounds produced by the different designs as described above. Responses were gathered from 32 subjects who were tested four at a time, in NASA Langley’s External Effects Room [10]. Each of the 99 sounds were played for 5 seconds. The subjects would then enter their subjective response on a tablet selecting from a continuous scale with verbal extremes ranging from “Not At All” annoyed to “Extremely” annoyed [11]. The sounds were played in a different, random, order for each of the 8 test sessions to remove possible bias due to test order. A summary of the test results follows.

<sup>5</sup> The HEAD Acoustics Artemis Suite of analysis tools was used to compute these metrics.

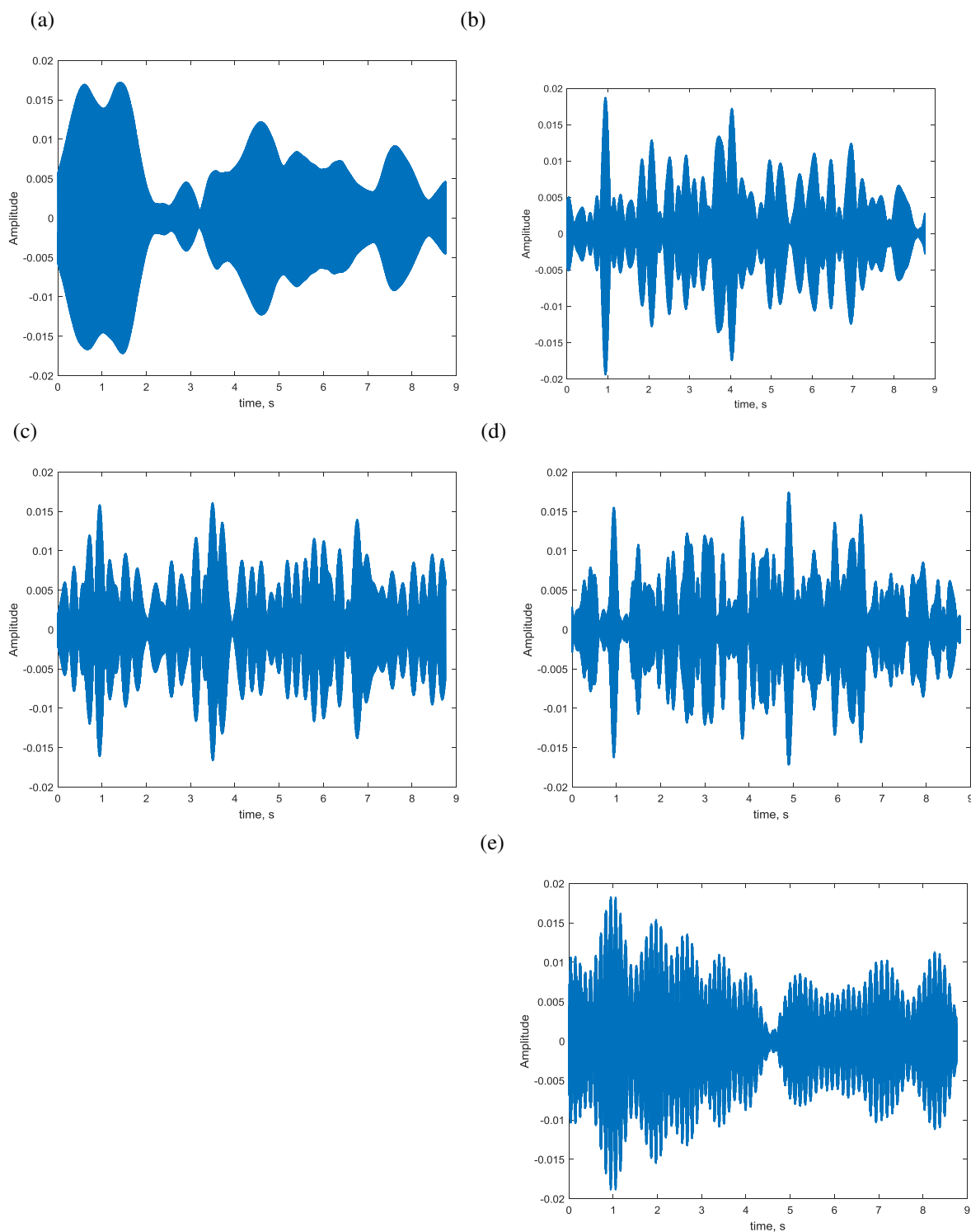


**Figure 13. Sample test sounds: (a) Realistic DF=0, (b) Realistic DF=1, (c) Loose control DF=0, (d) Loose control DF=1, (e) Realistic Random DF=1.**

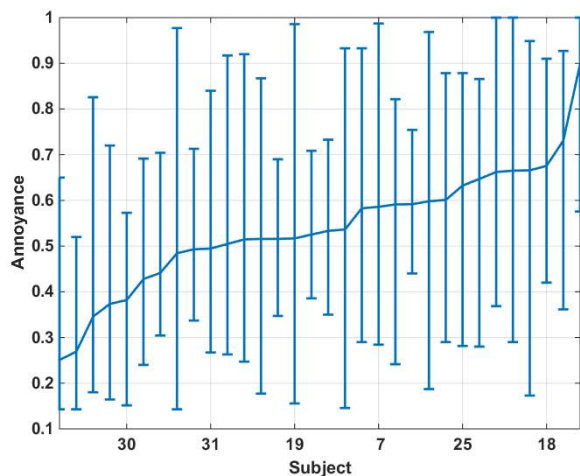


**Figure 14. Mean and range of normalized subject responses ordered by mean.**

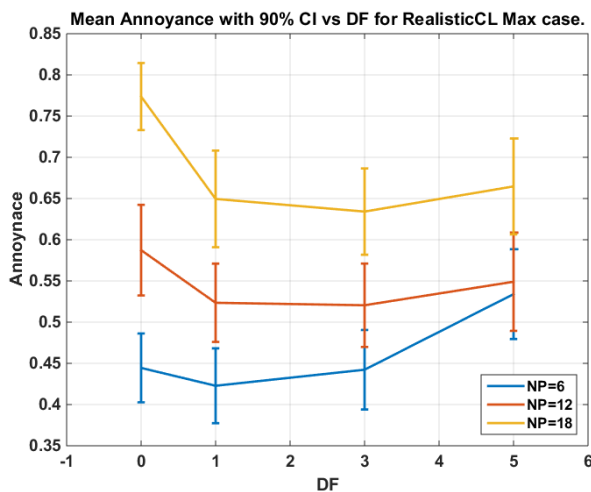


**Figure 15. Annoyance responses for Realistic sound class**

For NP=18, the Realistic Centerline and Realistic Sideline scored high for DF=0. The Loose Control class maintained a comparatively low and fairly constant annoyance level over the range of DF. It was hypothesized that the RandomDF class would mimic the Loose Control class, but this was not the case at higher levels of DF as the RandomDF design lacks the time varying phase attribute of the loose controller. In general, tightly controlled motors adversely affect annoyance at both extremes of the DF design space.

## VIII. Results

Normalized subject responses varied over a large range as illustrated in Figure 14. The means varied from about 0.25 to nearly 0.9. The range of a subject's response varied from a relatively tight  $\pm 0.15$  to nearly full scale ( $\pm 0.5$ ). Some subjects were not annoyed by most sounds and only moderately annoyed by a few. Other subjects were very annoyed by most sounds. The wide range of response is characteristic of this type of data and suggests that the data represents public opinion. It has been found over the years of testing that a sample size of around 30 subjects is adequate to produce repeatable results.

The annoyance responses for the Realistic sound class are shown in Figure 15. The error bars represent the 90% confidence interval of the data. The other sound classes are similar. A strong dependence on NP is evident. This was expected as the propellers were designed to have constant tip speed across all configurations. Recalling that the rpm must increase to keep tip speed constant at smaller diameters, it is straightforward to see that the Loudness, which in this range increases with frequency, would increase with NP, and, therefore, increase annoyance. It appears that the unmodulated sounds (DF=0) are, in general, more annoying than sounds with some modulation ( $1 \leq DF \leq 3$ ). Finally, there is little trend with DF except for NP=6, which shows noticeable increase in annoyance from DF=3 to DF=5.

The annoyance results for all sound classes for NP=6 and NP=18 are shown in Figure 16. The NP=12 result is similar and bounded by the NP=6 and NP=18 results. There are several things to note. First, the Ideal class returns higher annoyance than all the other sound classes. The Ideal class, with no randomization effects, would have the highest coherence between sources achieving the highest Loudness and degrees of modulation. For NP=6, both the Realistic Centerline and RandomDF classes scored high when DF=5.

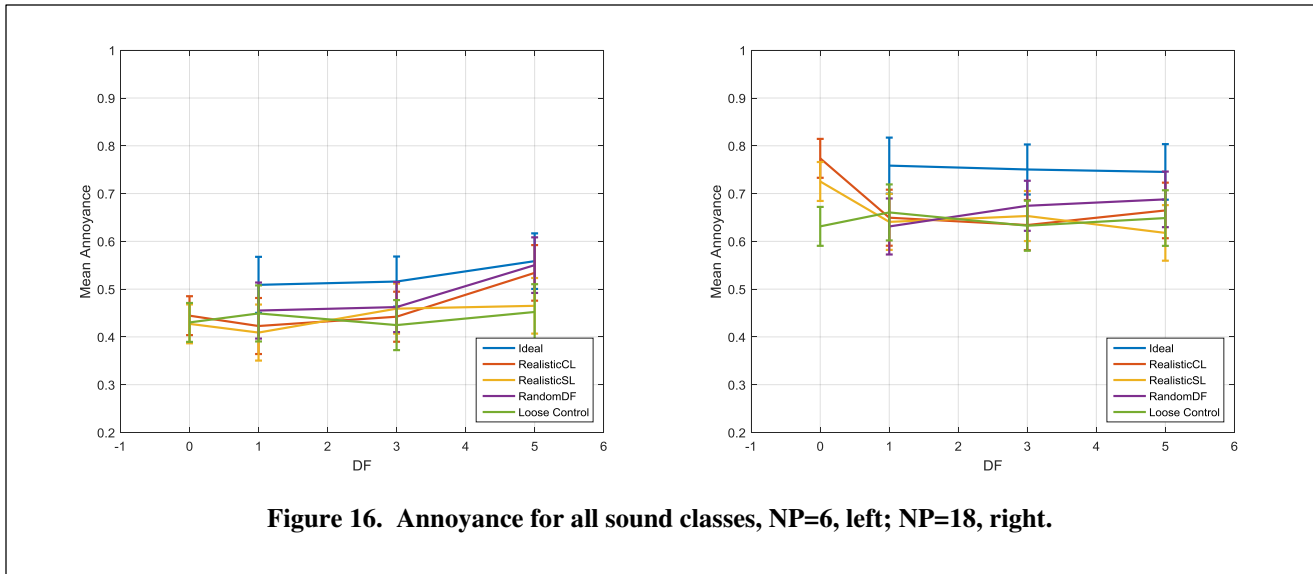


Figure 16. Annoyance for all sound classes, NP=6, left; NP=18, right.

## IX. Conclusions

The number of propellers is shown to be the dominant effect. Increasing the number of sources intensifies interference effects increasing level extremes spatially and temporally. The propeller rpm increases with the number of propellers translating the sound power produced to higher and, therefore, more annoying frequencies. The high annoyance recorded for the Ideal class demonstrates how high depths of modulation can increase annoyance. However, adding the randomization effects that would be present in real systems reduces the modulation enough so that some degree of modulation ( $1 \leq DF \leq 3$ ) is seen to be preferred over the more tonal  $DF = 0$  design. The phase variance introduced by a loose controller returns low annoyance figures in all configurations and may be the preferred design choice. The attempt to emulate loose control by rigidly randomizing the DF step appears to not work as well. The RandomDF class lacks the time varying phase modulation that is inherent in the Loose Control class.

The methodology employed has been shown to successfully inform the early design process of a Distributed Electric Propulsion system. Inserting noise analyses early in the design process is challenging for the designer, who has to learn new terminology and accept additional constraints, and the noise analyst, who must adapt his methods to provide timely results.

## X. References

- [1] M. D. Moore and B. Fredericks, "Misconceptions of Electric Aircraft and their Emerging Aviation Markets," in *52nd Aerospace Sciences Meeting*, National Harbor, MD, 2014.
- [2] A. M. Stoll, J. Bevirt, M. D. Moore, W. J. Fredericks and N. K. Borer, "Drag Reduction Through Distributed Electric Propulsion," in *14th AIAA Aviation Technology, Integration and Operations Conference*, Atlanta, 2014.
- [3] S. Okcu, "Psychoacoustic Analysis of Synthesized Jet Noise," Noise-Con 2013, Denver, CO, 2013.
- [4] ANSI S3-4.2007, "Procedure for the computation of Loudness of Steady Sounds," Acoustical Society of America, New York, 2007.
- [5] AIR 1407, "Prediction Procedure for Near-Field Propeller Noise," Society of Automotive Engineers, Inc, Warrendale, 1977.
- [6] V. E. Ostashev, D. Wilson and G. H. Goedecke, "Spherical wave propagation through inhomogeneous, anisotropic turbulence: Log-amplitude and phase correlations," *Acoustical Society of America*, vol. 115, no. 1, pp. 120-130, January 2004.
- [7] L. C. Nguyen and J. J. Kelly, "A Users Guide for the NASA ANOPP Propeller Analysis System," NASA CR 4768, Hampton, VA, 1997.

- [8] F. Farassat, "Linear Acoustic Formulas for Calculation of Rotating Blade Noise," *AIAA Journal*, vol. 19, no. 9, pp. 1122-1130, 1980.
- [9] L. Gutin, "On the Sound of a rotating Propeller," NASA TM1195, 1948.
- [10] K. J. Faller, "Acoustic Performance of a Real-Time Three-Dimensional Sound-Reproduction System," NASA/TM-2013-218004, 2013.
- [11] J. M. Fields and et al, "Standardized General-Purpose Noise Reaction Questions For Community Noise Surveys: Research and Recommendations," *Journal of Sound and Vibration*, vol. 242, no. 4, pp. 641-679, 2001.
- [12] T. Theodorsen and A. Regier, "The Problem of Noise Prediction with Reference to Light Airplanes," NASA TN 1145, 1946.